

## PAPER

# 'Maya chemistry' of organic–inorganic hybrid materials: isomerization, cyclicization and redox tuning of organic dyes attached to porous silicates†

Cite this: *RSC Adv.*, 2013, **3**, 20099

Antonio Doménech-Carbó,<sup>\*a</sup> Francisco M. Valle-Algarra,<sup>a</sup> María Teresa Doménech-Carbó,<sup>b</sup> Laura Osete-Cortina<sup>b</sup> and Marcelo E. Domine<sup>c</sup>

Association of indigo and lapachol dyes to aluminosilicate clays yields polyfunctional organic–inorganic hybrid materials forming Maya Blue-like systems. Upon partial removing of clay's zeolitic water by moderate thermal treatment, abundant isomerization, cyclicization and oxidation reactions occur defining a 'Maya chemistry' whose complexity could explain the versatile use of such materials in the pre-Columbian cultures and permits the preparation of polyfunctional materials potentially usable for therapeutic and catalytic purposes.

Received 11th June 2013

Accepted 16th August 2013

DOI: 10.1039/c3ra42890g

[www.rsc.org/advances](http://www.rsc.org/advances)

## Introduction

Maya Blue, an ancient nanostructured material obtained upon attachment of indigo dye to phyllosilicate clays by ancient Mesoamerican peoples in pre-Columbian times can be considered as a precursor of contemporary hybrid organic–inorganic materials.<sup>1</sup> The study of the composition and structure of such historic materials is of interest not only for their high archaeological and ethnohistoric value, but also their implications for modern synthesis of hybrid materials having applications as optical carriers, polymer reinforcement, paints and pigments, photonic antennas and photosensitizers.<sup>2</sup>

Although there is controversy surrounding the nature of the clay–dye association and the location of dye molecules in the clay framework,<sup>3</sup> the most extended view on such hybrid materials considers them as constituted exclusively by molecules of the parent dye distributed externally and/or in pores and channels of the clay.<sup>4</sup>

Contrary to this view, we proposed that dehydroindigo (DHI), the oxidized form of indigo, accompanies this dye as a minority – but in significant proportion – component of Maya Blue contributing to the peculiar variability in the pigment hue, which ranges from the blue to turquoise greenish blue.<sup>5</sup> Recent archaeological discoveries permitted to detect other

associations between clays and indigoid dyes in the area Maya, suggesting that there was a 'Maya chemistry' no limited to the Maya Blue.<sup>6</sup> This chemistry would be characterized by the polyfunctional nature of the involved hybrid materials, where different organic components, in particular those resulting from redox tuning of the parent dye, exist (Fig. 1).<sup>3,7</sup> Although this view has been supported by photochemical studies from Rondao *et al.*,<sup>8</sup> TDDFT calculations from Tilocca and Fois<sup>9</sup> and studies of Giustetto *et al.*<sup>10</sup> on different dye@clay materials, it has been more or less explicitly questioned in other recent literature. In particular, Sánchez del Río *et al.*,<sup>11</sup> Martinetto *et al.*,<sup>12</sup> Giulieri *et al.*,<sup>13</sup> Chryssikos *et al.*<sup>14</sup> and Lima *et al.*,<sup>15</sup> who studied different indigo@support materials with high dye loadings (until 20% wt) do not find dye molecules other than the parent indigo. In this context, several questions arise: among others, if there is effectively formation of oxidized indigo



**Fig. 1** Green pellets from La Blanca archaeological site in Guatemala.<sup>7b</sup> A clay plus dye material containing dehydroindigo as a majority organic component.

<sup>a</sup>Departament de Química Analítica, Universitat de València, Dr Moliner, 50, Burjassot, València, 46100, Spain. E-mail: antonio.domenech@uv.es

<sup>b</sup>Institut de Restauració del Patrimoni, Universitat Politècnica de València, Camí de Vera 14, 46022, València, Spain

<sup>c</sup>Instituto de Tecnología Química, ITQ (Universitat Politècnica de València – CSIC) Avda, Los Naranjos S/N, 46022, Valencia, Spain

† Electronic supplementary information (ESI) available: Scanning electron microscopy images of specimens, voltammograms, Vis-UV spectra, UPLC-MS, Py-GC-MS and mass spectra and detailed descriptions of experimental procedures are provided. See DOI: 10.1039/c3ra42890g

forms in indigo@support materials, if this formation occurs only under very definite conditions and if the possibility of this kind of processes is restricted to indigo.

The purpose of the current report is to provide experimental evidence on the existence of different reactions affecting the dye component, including redox tuning, during the preparation of Maya Blue type dye@clay materials. For this purpose, it has been studied the composition of materials prepared upon attachment to phyllosilicate clays of two dyes, historically used as colorants by ancient Mesoamerican peoples,<sup>16</sup> indigotin or indigo (3*H*-indol-3-one-2-(1,3-dihydro-3-oxo-2*H*-indol-2-ylidene)-1,2-dihydro-(2*E*)), extracted from leaves of *añil* or *xiuquilitl* (*Indigofera suffruticosa*) and lapachol (2-hydroxy-3-(3-methyl-2-butenyl)-1,4-naphtho-quinone), extracted from *guatechupin* plant (*Diphysa robinoides*, fam. *Fabaceae*). Complexes of such dyes with palygorskite and sepiolite, fibrous phyllosilicates of ideal compositions  $\text{Si}_8(\text{Mg}_2\text{Al}_2)\text{O}_{20}(\text{OH})_2(\text{H}_2\text{O})_4 \cdot 4\text{H}_2\text{O}$ , and  $\text{Si}_6\text{Mg}_4\text{O}_{15}(\text{OH})_2 \cdot 6\text{H}_2\text{O}$ , respectively, have been studied from combination of solid state electrochemistry and adsorptive voltammetry techniques together with high performance liquid chromatography with diode array detection (LC-DAD), ultra performance liquid chromatography coupled with mass spectrometry (UPLC-MS) and pyrolysis-silylation gas chromatography-mass spectrometry (Py-GC-MS), combined with electron microscopy, visible and infrared spectroscopies.

It should be emphasized that the association between dye and the 'internal' walls of the clay pores/channels can be considered as the key point determining the stability of the Maya Blue type materials, and adsorption on the external surfaces plays only a minor role. The essential idea, in agreement with previous results on indigo plus palygorskite specimens,<sup>5-7</sup> is that this association involves the appearance of a significant proportion of oxidized forms (dehydroindigo and isatin in the case of indigo-based materials, dehydrolapachones in the case of lapachol-based ones), accompanied by other organic components. All these oxidised compounds are ubiquitous components of genuine Maya Blue-type materials prepared with 'historical' indigo loadings (1% wt) in clay.

On the other hand, the stabilization of different organic components in the prepared hybrid materials could be of interest also from the ethnohistorical and biomedical points of view because lapachol,<sup>17</sup> and lapachones<sup>18</sup> as well as isatin<sup>19</sup> derivatives exhibit antitumor, antibiotic, antimalarial, anti-inflammatory and antiulceric activities. In fact, palygorskite was used for therapeutic purposes in the rich Maya medicine.<sup>20</sup>

## Experimental

Dye@clay specimens were prepared by 60 min crushing dye (1% w/w)-clay mixtures and subsequent application of thermal treatment in furnace between 100 and 180 °C for times between 15 min and 24 h. Thermal treatment, producing the partial loss of zeolitic water of the clays, is a precondition to obtain stable pigmenting materials having a strong dye-clay association.<sup>2-5</sup> However, it should be emphasized that a fraction of the dye remains externally adsorbed to the clay matrix, and that is extracted by organic solvents. Here, conventional extraction was

performed with different organic solvents and solvent mixtures during 10 h. Such extracts were analyzed by LC-DAD, UPLC-MS and Py-GC-MS using instrumentation and procedures described as ESI.<sup>†</sup> <sup>1</sup>H and <sup>13</sup>C NMR spectra were obtained from deuterated DMSO extracts. The dye@clay specimens were characterized by XRD, transmission electron microscopy (TEM) ATR-FTIR and Vis-UV diffuse reflectance spectroscopy. Solid state voltammetric techniques, based on the voltammetry of microparticles approach developed by Scholz *et al.*,<sup>21</sup> were applied as previously reported,<sup>5-7</sup> and complemented here with electrochemical impedance spectroscopy (EIS) and scanning electrochemical microscopy (SECM).

## Results and discussion

### Indigo@clay hybrids

Fig. 2 compares DMSO extraction experiments on indigo@sepiolite specimens prepared at 25 °C and treated at 150 °C during 24 h (IN@SP<sub>25</sub> and IN@SP<sub>150</sub>, respectively). The extract from the non-heated sample exhibits an intense blue color due to indigo accompanied by a low proportion of isatin. In contrast, heated specimens produced almost colorless extracts where dehydroindigo accompanies indigo and isatin, the dehydroindigo/indigo ratio increasing on increasing the temperature of preparation of the specimen. Remarkably, the sepiolite and palygorskite materials remain intensely turquoise blue after extraction, thus denoting that the dye molecules are strongly attached to the inorganic support. This is a difference with materials prepared with laminar clays such as kaolinite and montmorillonite,<sup>7d</sup> where extraction with organic solvents removes entirely the dye. Fig. 2 also shows the LC-DAD chromatogram ( $\lambda = 254 \text{ nm}$ ) for the DMSO extract (10 h) of IN@SP<sub>150</sub> sample where indigo, dehydroindigo and isatin peaks can be seen. Such dyes were identified from Vis-UV spectra of fractions (see ESI<sup>†</sup>), as well as their MS spectra (see Fig. 2) from equivalent UPLC-MS experiments. <sup>1</sup>H and <sup>13</sup>C NMR spectra from DMSO extracts agreed with those reported in literature for indigo,<sup>22</sup> dehydroindigo<sup>8a</sup> and isatin.<sup>23</sup> Identification of

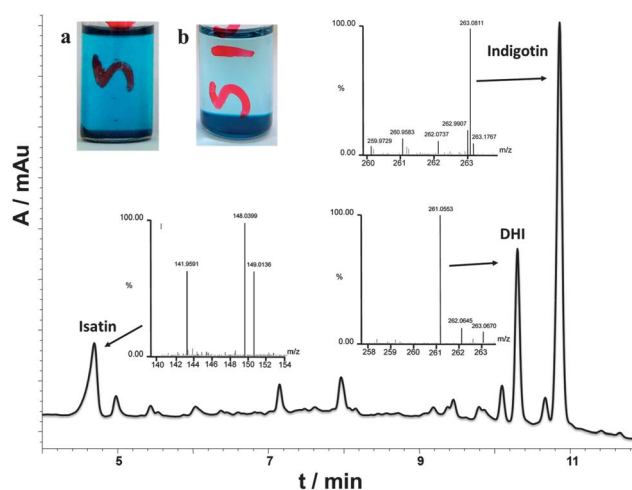


**Fig. 2** LC-DAD chromatogram ( $\lambda = 254 \text{ nm}$ ) for DMSO extract. Insets: mass spectra of IN@SP<sub>150</sub> specimen heated at 150 °C recorded in UPLC-MS experiments. Photographic Images of DMSO extraction vials for (a) IN@SP<sub>25</sub> and (b) IN@SP<sub>150</sub> specimens.

those components was confirmed by their  $^1\text{H}$  and  $^{13}\text{C}$  NMR signatures in ESI.† The prepared specimens also displayed TEM images and spectral signatures (ATR-FTIR, Vis-UV) coincident with those previously reported.<sup>6</sup>

Solution phase electrochemistry confirmed the presence of dehydroindigo and isatin accompanying indigo in the DMSO extracts from indigo@palygorskite (IN@PL) and indigo@sepiolite (IN@SP) specimens while, in agreement with previous results,<sup>5,6</sup> and with our recent spectral and voltammetric data,<sup>24</sup> solid state voltammetry denoted the presence of such components in the materials and confirmed the increase in the dehydroindigo/indigo ratio on increasing the temperature of the thermal treatment used in the preparation of the specimens. This is based on characteristic voltammetric signatures corresponding to the oxidation of indigo to dehydroindigo (at +0.45 V vs. Ag/AgCl in aqueous acetate buffer) and the reduction of indigo to leucoindigo (at -0.30 V in the indicated conditions) described for indigo<sup>25</sup> and Maya Blue samples.<sup>5-7</sup>

We present here additional data based on electrochemical impedance spectroscopy (EIS) and scanning electrochemical microscopy (SECM). Fig. 3 compares the impedance spectra of IN@PL (specimens unheated, IN@PL<sub>25</sub>, and treated at 150 °C during 10 h, IN@PL<sub>150</sub>) attached to graphite electrodes in contact with a  $\text{Fe}(\text{CN})_6^{3-}/\text{Fe}(\text{CN})_6^{4-}$  solution in aqueous acetate buffer. Applying a bias potential above +0.20 V vs. Ag/AgCl, the EIS spectra reflects the response of the modified electrode to the electrochemical oxidation of hexacyanoferrate(II) ion, which acts as a redox probe. When this potential is not high enough to promote the oxidation of indigo to dehydroindigo, both unheated and heated materials yield essentially identical Nyquist and Bode plots; however, when the bias potential is sufficiently larger to promote the additional oxidation of indigo to dehydroindigo, significant differences appear between such specimens, as can be seen in Fig. 3.

These results can be rationalized on considering that the unheated specimen contains predominantly indigo externally

attached to the clay support with dehydroindigo almost entirely absent. While, in the heated specimens, the dye molecules are predominantly located in 'internal' clay sites and a significant proportion of dehydroindigo exists. At a potential of +0.25 V, where no oxidation of indigo to dehydroindigo occurs, the response of the  $\text{Fe}(\text{CN})_6^{3-}/\text{Fe}(\text{CN})_6^{4-}$  redox probe was almost identical for both materials only reflecting minimal differences in porosity of the layered materials. When a potential of +0.45 V is applied, the oxidation of indigo to dehydroindigo occurs and now the difference in the composition of the specimens results in significant differences in their EIS spectra.

Similar results were obtained at the micrometer level using SECM, a technique providing topographic information on electrochemical reactivity,<sup>26</sup> again with the help of the  $\text{Fe}(\text{CN})_6^{3-}/\text{Fe}(\text{CN})_6^{4-}$  redox probe. Experiments in Fig. 4 were performed following methods for examining microparticulate deposits<sup>26b</sup> using redox competition mode.<sup>26c</sup> Here, microparticulate deposits of IN@PL<sub>25</sub> and IN@PL<sub>150</sub> on a graphite substrate electrode were submitted to different potentials ( $E_s$ ), whereas the tip electrode was maintained at a potential sufficiently positive ( $E_T$ ) to oxidize  $\text{Fe}(\text{CN})_6^{4-}$ . In these conditions, peaked topographies were recorded, corresponding to the sharp variation of the substrate conductivity when the tip passes from the vicinity of the bare graphite to the regions occupied by the clay grains. In the case of heated IN@PL and IN@SP specimens, the SECM topography remained essentially unchanged when the substrate potential was moved from 0.00 to +0.45 V, as can be seen in Fig. 4a and b for IN@PL<sub>150</sub>. For unheated specimens, however, the topography changed significantly upon performing such change in  $E_s$ , as illustrated in Fig. 4c and d for IN@PL<sub>25</sub>. These results can be again rationalized on considering that there is a significant proportion of indigo available to be electrochemically oxidized in unheated specimens, while the dye is less accessible to electrochemical oxidation in thermally treated specimens.

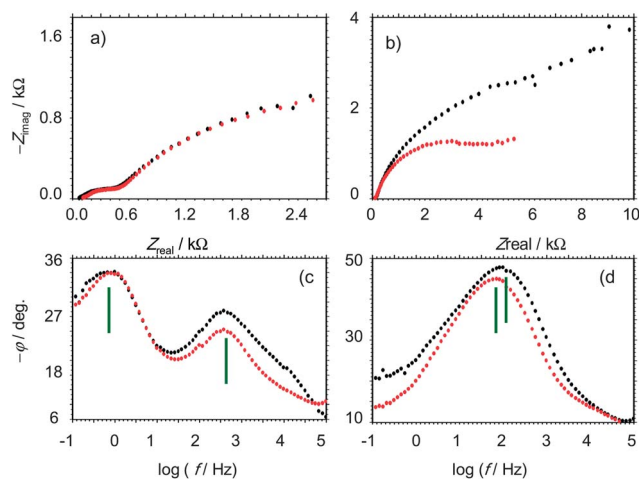


**Fig. 3** Nyquist (a and b) and Bode (c and d) plots for EIS spectra of IN@PL<sub>25</sub> (black points) and IN@PL<sub>150</sub> (red points) specimens attached to graphite electrodes in contact with 2.5 mM  $\text{K}_4\text{Fe}(\text{CN})_6$  + 2.5 mM  $\text{K}_3\text{Fe}(\text{CN})_6$  solution in 0.25 M HAc/NaAc, pH 4.75. Applied potential: (a and c) +0.25 V; (b and d) +0.45 V.

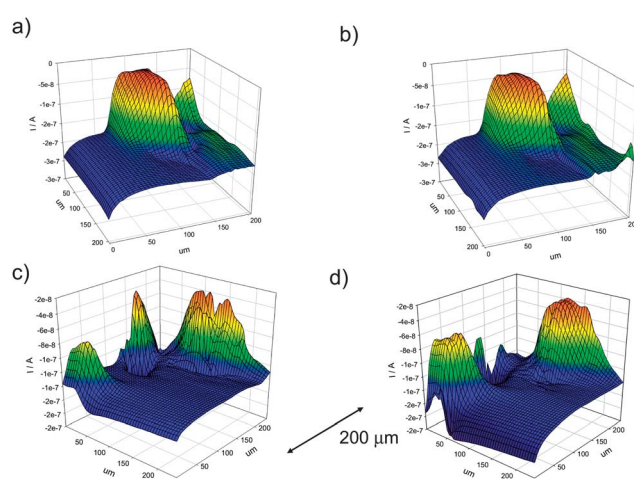


**Fig. 4** SECM experiments for (a and b) IN@PL<sub>150</sub> and (c and d) IN@PL<sub>25</sub> specimens attached to graphite plate in contact with 0.25 M HAc/NaAc containing 2.0 mM  $\text{K}_4\text{Fe}(\text{CN})_6$  as a redox probe.  $E_T = +0.30$  V; (a and c)  $E_s = 0.00$  V; (b and d)  $E_s = +0.45$  V.

It is pertinent to emphasize that the preparation of the historical pigment, due to the absence of historical sources describing it, remains unknown.<sup>27</sup> Despite of that, different preparation recipes in particular involving vat dyeing techniques, have been proposed for laboratory studies.<sup>15</sup> In general, the 'dry' preparation of Maya Blue-type materials *via* grinding of a mixture of the solid dye and the clay, followed by subsequent heating at temperatures between 100 and 200 °C is used.<sup>3,4</sup> The type of preparation and the dye loading plays a crucial role; in fact, most of Maya Blue-type materials recently prepared<sup>9</sup> involve indigo loadings larger (until 20% wt) than the theoretical maximum channel occupation in palygorskite (*ca.* 4% wt),<sup>28</sup> and the considered as typical value for 'historical' Maya Blue (*ca.* 1% wt).<sup>7,4,11b</sup> In these circumstances, it appears that the majority of the organic component remains as 'external' microparticulate deposit<sup>12a</sup> and that redox tuning reactions become masked.

### Lapachol@clay hybrids

Preparation of lapachol plus palygorskite and sepiolite clays (LA@PL and LA@SP) resulted in features comparable to those for their indigo counterparts. The composition of methanol extracts from lapachol@clay mixtures was significantly dependent on the temperature of the thermal treatment. This can be seen in the chromatograms shown in Fig. 5 for lapachol, thermally treated lapachol, and thermally treated lapachol plus palygorskite and sepiolite specimens. Contrary to indigo, which remains thermally stable until 380 °C,<sup>4a</sup> lapachol decomposes at temperatures above 120 °C, giving rise to a complex mixture of products. The chromatogram of lapachol solution as well as those for the unheated mixtures of the dye with tested clays (non-represented), provides a unique chromatographic peak corresponding to the elution of the

parent dye. In contrast, application of thermal treatment above 150 °C during 24 h leads to extracts where the lapachol peak is practically absent and replaced by peaks for several lapachones and dehydrolapachone. This means that, even externally adsorbed, attachment to the clay blocks the thermal decomposition of the dye and the extract consists of a 'clean' mixture of products resulting from isomerization/cyclization ( $\alpha$ -lapachone and other isomers, 4-hydroxy- $\alpha$ -lapachone, dihydro-4-hydroxy- $\alpha$ -lapachone) and oxidation (dehydro- $\alpha$ -lapachone), identified from their <sup>1</sup>H and <sup>13</sup>C NMR signatures and mass spectra in UPLC-MS experiments (see ESI†). Three features should be underlined: (i) such chromatographic changes only appear after thermal treatment; (ii) blank experiments heating solid lapachol samples yield partial lapachol decomposition but rather different compounds are formed; (iii) after equivalent thermal treatment, palygorskite and sepiolite clays yield similar, but non-coincident products.

The possibility of redox tuning was confirmed from solid state electrochemistry and conventional voltammetry of lapachol solution and adsorbed on glassy carbon electrode from extracts of LA@PL and LA@SP specimens on 90 : 10 (v/v) H<sub>2</sub>O : DMSO. The cyclic voltammograms of both microparticulate deposits of LA@PL and LA@SP and their extracts display similar features in contact with aqueous acetate buffer, as can be seen in Fig. 6.

Lapachol and lapachol plus clay specimens provide overlapping cathodic peaks at -0.30 V and an apparently irreversible anodic peak at +0.85 V. In agreement with quinone<sup>29</sup> lapachol<sup>30</sup> electrochemistry literature, the cathodic process can be attributed to the quinone reduction to catechol of the parent lapachol. Remarkably, the oxidation peak becomes significantly diminished until it entirely vanishes for thermally treated specimens. This feature suggests that a significant portion of the parent lapachol has been oxidized in thermally treated dye plus clay mixtures. This clay-assisted oxidation mimics that observed in the biochemical context.<sup>31</sup> Consistently, in the cathodic scans subsequent to the oxidation of lapachol to dehydrolapachol, this

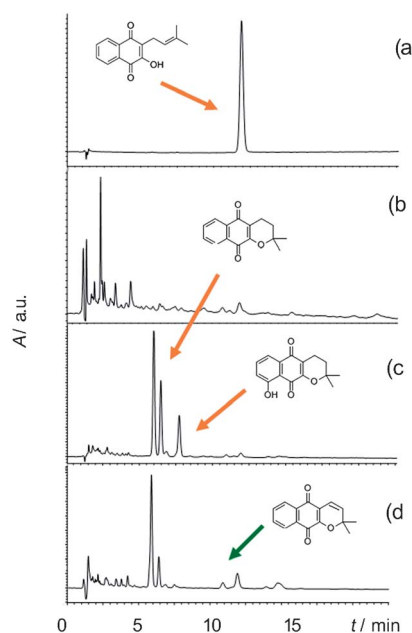


**Fig. 5** LC-DAD chromatograms for MeOH solutions of (a) lapachol and (b) lapachol treated at 150 °C during 10 h, and the MeOH extracts (24 h contact) of (c) LA@PL<sub>150</sub> and (d) LA@SP<sub>150</sub>. Detector wavelength 254 nm.

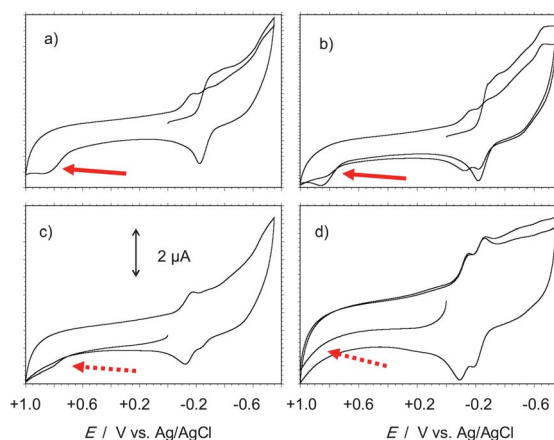


**Fig. 6** Cyclic voltammograms of (a and b) LA@P; (c and d) LA@P150 specimens using: (a and c) extracts on 90 : 10 (v/v) H<sub>2</sub>O : DMSO adsorbed onto glassy carbon electrode; (b and d) solid microsamples attached to paraffin-impregnated graphite electrodes, all immersed into 0.25 M aqueous sodium acetate buffer, pH 4.75. Potential scan rate 50 mV s<sup>-1</sup>.

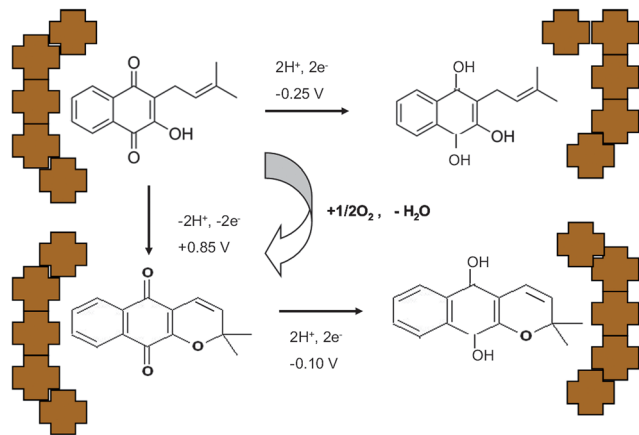


**Fig. 7** Schematic for the main chemical and electrochemical cyclization and oxidation processes involving LA@PLT specimens.

last compound is electrochemically reduced, *via* quinone to catechol, at potentials close to that of the parent lapachol, giving rise to peak splitting in the 0.0 to  $-0.4$  V potential range. Fig. 7 shows the proposed reaction scheme.

### Advocating ‘Maya chemistry’

The reported results indicate that: (i) upon attachment to microporous clay supports, indigo and lapachol dyes experience selected cyclization and oxidation reactions; (ii) the reactions are prompted by the loss of zeolitic water and evidence the strong attachment of the dyes to the clay framework. It should be underlined that the observation of these reactions requires the use of dye loadings of *ca.* 1% wt, just those estimated in genuine Maya Blue samples and below the theoretical maximum loading (*ca.* 4% wt) for filling clay channels.<sup>7d</sup> Such processes, however, become masked in materials prepared at high dye loadings, where the majority of the dye remains adsorbed or forming microparticulate deposits external to the clay support, as is the case of most of recent literature.<sup>11–15</sup>

Accordingly, it can be proposed that a ‘Maya chemistry’, based on the combination of dyes and clays under the aforementioned conditions (*ca.* 1% wt dye, thermal treatment between 100 and 180 °C) yields nanostructured, polyfunctional organic–inorganic hybrid materials where the parent organic component is accompanied by other components resulting from isomerization/cyclization and redox reactions. Importantly, such reactions occur only *via* dye attachment to the clay support which could provide catalytic sites for isomerization/cyclization and oxidation reactions experienced by the dyes. As far as a portion of the organic components produced in such reactions become extractable by organic solvents, it appears that the parent dye could experience the aforementioned reactions upon attachment to different support (both ‘internal’ both ‘external’) sites. In the case of the indigo- and lapachol-based materials studied here, dye attachment to the ‘internal’ walls of clay pores, prompted by the required evacuation of zeolitic water upon heating, appears as the essential requirement for obtaining materials where organic components become stabilized. In this view, the (organic) multicomponent nature was

consubstantial of the ‘Mayan’ materials so that, the prepared indigo plus clay materials at high dye loadings could not be considered as ‘Mayan’ materials *sensu stricto*.

In this view, and in agreement with previous reports,<sup>5–7,24</sup> the composition of the system (in particular the dehydroindigo/indigo ratio in Maya Blue) can be modulated by varying the temperature of thermal treatment. The variable proportion of dehydroindigo could explain the peculiar hue variability of the Maya Blue and suggest that different preparative recipes were used during the Mayan times.<sup>5</sup> Accordingly, the ancient Mesoamerican people anticipated, possibly, not only contemporary organic–inorganic hybrid materials, but also, thermal control of reactivity.<sup>5c</sup>

Another aspect of interest is that several of the compounds resulting from cyclization and redox tuning reactions, have biomedical interest. In fact, lapachol and several isomers and derivatives exhibit antitumor, antibiotic, antimalarial, anti-inflammatory and antiulceric activities,<sup>17</sup> in particular, dehydrolapachone exhibits antivasular activity.<sup>18</sup> In turn, isatin possesses antiviral, antitumor and antiangiogenic, antibacterial, antitubercular, antifungal, antiapoptotic, anticonvulsant and anxiolytic activities.<sup>19</sup> In this regard, it should be emphasized that: (i) attachment of lapachol and indigo to clays supports determines ‘clean’ synthesis where a limited number of products (see Fig. 2 and 5) is formed under easily controllable conditions; (ii) a significant portion of the synthesized compounds becomes externally adsorbed to the clay crystals and is easily extracted, so that such compounds become available for dosage/administration purposes in the biomedical context. These characteristics could be exploited in pharmacological applications.

Were the ancient Mayas aware of the capabilities of the dye@clay associations? Could the ancient Mesoamericans exploit the therapeutic possibilities of these polyfunctional hybrid materials? The recent discovery of a set of greenish pellets in the site of La Blanca (Terminal Classic period, *ca.* 800–950 AD) in Guatemala, appearing as an ancient palygorskite plus dye plaster (Fig. 1),<sup>6b</sup> dominated by dehydroindigo, would reflect the use of dye plus clay materials in a quotidian (decorative?, pharmacological?) context.

The possibility of therapeutic use of such materials by ancient Mesoamerican people, would be open on considering the rich ‘Maya Blue’ synthetic chemistry developed by the Mesoamerican peoples and the equally rich Mayan pharmacopea,<sup>32</sup> but has to be supported by archaeological and ethno-historical data.

## Conclusions

Organic–inorganic hybrid dye@clay materials prepared from indigo and lapachol, and palygorskite and sepiolite at dye loadings *ca.* 1% wt can be considered as nanostructured polyfunctional materials in which dye attachment to the clay channels determines abundant isomerization/cyclization and redox tuning reactions. In particular, oxidized forms of the parent dye, namely, dehydroindigo and isatin from indigo, and dehydrolapachone from lapachol, become stabilized upon attachment to the inorganic support.

It is advocated the view that genuine – in the historical meaning – Maya Blue-type materials are just characterized by their multicomponent, polyfunctional, nature. Within this view, there is possibility of defining a ‘Maya chemistry’ where a variety of organic products – among them, those potentially usable for therapeutic purposes – could be easily synthesized.

## Acknowledgements

Financial support is gratefully acknowledged from the MEC Projects CTQ2011-28079-CO3-01 and 02 which are also supported with ERDF funds.

## Notes and references

- 1 P. Romero and C. Sánchez, *New J. Chem.*, 2005, **29**, 57–58.
- 2 G. Calzaferri, S. Huber, H. Maas and C. Minkowski, *Angew. Chem.*, 2003, **42**, 3732–3758.
- 3 A. Doménech, M. T. Doménech, M. Sánchez del Río, M. Vázquez and E. Lima, *New J. Chem.*, 2009, **33**, 2371–2379.
- 4 (a) B. Hubbard, W. Kuang, A. Moser, G. A. Facey and C. Detellier, *Clays Clay Miner.*, 2003, **51**, 318–326; (b) E. Fois, A. Gamba and A. Tilocca, *Microporous Mesoporous Mater.*, 2003, **57**, 263–272; (c) M. Sánchez del Río, P. Martinetto, A. Somogyi, C. Reyes-Valerio, E. Dooryhée, N. Peltier, L. Alianelli, B. Moignard, L. Pichon, T. Calligaro and J.-C. Dran, *Spectrochim. Acta, Part B*, 2004, **59**, 1619–1625; (d) R. Giustetto, F. X. Llabres i Xamena, G. Ricchiardi, S. Bordiga, A. Damin, R. Gobetto and M. R. Chierotti, *J. Phys. Chem. B*, 2005, **109**, 19360–19368.
- 5 (a) A. Doménech, M. T. Doménech and M. L. Vázquez, *J. Phys. Chem. B*, 2006, **110**, 6027–6039; (b) A. Doménech, M. T. Doménech and M. L. Vázquez, *J. Phys. Chem. C*, 2007, **111**, 4585–4595; (c) A. Doménech, M. T. Doménech and M. L. Vázquez, *Anal. Chem.*, 2007, **79**, 2812–2821; (d) A. Doménech, M. T. Doménech and M. L. Vázquez, *Archaeometry*, 2009, **51**, 1015–1034.
- 6 (a) A. Doménech, M. T. Doménech and M. L. Vázquez, *Angew. Chem., Int. Ed.*, 2011, **50**, 5741–5744; (b) A. Doménech, M. T. Doménech, C. Vidal and M. L. Vázquez, *Angew. Chem., Int. Ed.*, 2012, **51**, 700–703.
- 7 (a) A. Doménech, M. T. Doménech, M. Sánchez del Río, E. Goberna and E. Lima, *J. Phys. Chem. C*, 2009, **113**, 12118–12131; (b) A. Doménech, M. T. Doménech, M. Sánchez del Río and M. L. Vázquez, *J. Solid State Electrochem.*, 2009, **13**, 869–878; (c) A. Doménech, M. T. Doménech, F. Valle, M. E. Domine and L. Osete, *J. Mater. Sci.*, 2013, **48**, 7171; (d) A. Doménech, F. Valle, M. T. Doménech, M. E. Domine, L. Osete and J. V. Gimeno, *ACS Appl. Mater. Interfaces*, DOI: 10.1021/am402193u.
- 8 (a) R. Rondao, J. S. De Melo, B. D. Bonifacio and M. J. Melo, *J. Phys. Chem. A*, 2010, **114**, 1699–1708; (b) R. Rondao, J. S. Seixas de Melo and G. Voss, *ChemPhysChem*, 2010, **11**, 1903–1908.
- 9 A. Tilocca and E. Fois, *J. Phys. Chem. C*, 2009, **113**, 8683–8687.
- 10 (a) R. Giustetto, K. Seenivasan, F. Bonino, G. Ricchiardi, S. Bordiga, M. R. Chierotti and R. Gobetto, *J. Phys. Chem. C*, 2011, **115**, 16764–16776; (b) R. Giustetto and O. Wahyudi, *Microporous Mesoporous Mater.*, 2011, **142**, 221–235; (c) R. Giustetto, K. Seenivasan, D. Pellerej, G. Ricchiardi and S. Bordiga, *Microporous Mesoporous Mater.*, 2012, **155**, 167–176.
- 11 (a) M. Sánchez del Río, E. Boccaleri, M. Milanesio, G. Croce, W. van Bee, Nad and C. Tsiantos, *J. Mater. Sci.*, 2009, **44**, 5524–5536; (b) C. Mondelli, M. Sánchez del Río, M. A. González, A. Magazzú, C. Cavalleri, M. Suárez, E. García-Romero and P. Romano, *J. Phys.: Conf. Ser.*, 2012, **340**, 1–6.
- 12 (a) C. Dejoie, P. Martinetto, E. Dooryhée, P. Strobel, S. Blanca, P. Bordat, R. Brown, F. Porcher, M. Sanchez del Rio and M. Anne, *ACS Appl. Mater. Interfaces*, 2010, **2**, 2308–2316; (b) C. Dejoie, P. Martinetto, E. Dooryhée, R. Brown, S. Blanc, P. Bordat, P. Strobel, P. Odier, F. Porcher, M. Sanchez del Rio, E. Van Eslande, P. Walter and M. Anne, *Mater. Res. Soc. Symp. Proc.*, 2011, **1319**, 103–115.
- 13 (a) S. Ovarlez, F. Giulieri, A.-M. Chaze, F. Delamare, J. Raya and J. Hirschinger, *Chem.–Eur. J.*, 2010, **15**, 11326–11332; (b) S. Ovarlez, F. Giulieri, F. Delamare, M. Sbirrazzuoli and A.-M. Chaze, *Microporous Mesoporous Mater.*, 2011, **142**, 371–380; (c) F. Giulieri, S. Ovarlez and A.-M. Chaze, *Int. J. Nanotechnol.*, 2012, **9**, 605–617.
- 14 C. Tsiantos, M. Tsampodimou, G. H. Kacandes, M. Sánchez del Río, V. Gionis and G. D. Chryssikos, *J. Mater. Sci.*, 2012, **47**, 3415–3428.
- 15 E. Lima, A. Guzmán, M. Vera, J. L. Rivera and J. Fraissard, *J. Phys. Chem. C*, 2012, **116**, 4556–4563.
- 16 M. E. Haude, *Identification and Classification of Colorants Used During Mexico's Early Colonial Period*, The American Institute for Conservation, 1997, vol. 60, p. 1.
- 17 Y. Kumagai, Y. Tsurutani, M. Shinyashiki, S. H. Takeda, Y. Nakai, T. Yoskikawa and N. Shimojo, *Environ. Toxicol. Pharmacol.*, 1997, **3**, 245–250.
- 18 (a) H. R. Nasiri, M. Bolte and H. Schwalbe, *Nat. Prod. Res.*, 2008, **22**, 1225–1230; (b) I. Garkavtsev, V. P. Chauhan, H. K. Wong, A. Mokhopadhyay, M. A. Glicksman, R. T. Peterson and R. K. Jain, *Proc. Natl. Acad. Sci. U. S. A.*, 2011, **108**, 11596–11601.
- 19 A. Medvedev, O. Buneeva and V. Glover, *Biologics*, 2007, **1**, 151–162.
- 20 D. E. Arnold, J. R. Branden, P. R. Williams, G. M. Feinman and J. P. Brown, *Antiquity*, 2008, **82**, 152–164.
- 21 (a) F. Scholz, U. Schröder and R. Gulabovskii, *Electrochemistry of Immobilized Particles and Droplets*, Springer, Berlin-Heidelberg, 2005; (b) A. Doménech, J. Labuda and F. Scholz, *Pure Appl. Chem.*, 2013, **85**, 609–632.
- 22 R. C. Hoffman, R. C. Zilber and R. E. Hoffman, *Magn. Reson. Chem.*, 2010, **48**, 892–895.
- 23 (a) H. Laatsch, R. H. Thomson and P. J. Cox, *J. Chem. Soc., Perkin Trans. 2*, 1984, 1331; (b) J. F. M. da Silva, S. J. Garde and A. C. Pinto, *J. Braz. Chem. Soc.*, 2001, **12**, 273–324.
- 24 (a) A. Doménech, M. Martini, L. M. de Carvalho and M. T. Doménech, *J. Electroanal. Chem.*, 2012, **684**, 13–19; (b) A. Doménech, M. T. Doménech, L. Osete and N. Montoya, *Microporous Mesoporous Mater.*, 2013, **166**, 123–130.

- 25 (a) A. M. Bond, F. Marken, E. Hill, R. G. Compton and H. Hügel, *J. Chem. Soc., Perkin Trans. 2*, 1997, 1735–1742; (b) J.-B. He, G.-H. Ma, J.-C. Chen, Y. Yao and Y. Wang, *J. Electroanal. Chem.*, 2010, **55**, 4845–4850.
- 26 (a) *Electrochemical Microscopy*, ed. A. J. Bard and M. V. Mirkin, Taylor & Francis, Boca Raton, 2001; (b) H. He, Z. Ding and D. W. Shoesmith, *Electrochem. Commun.*, 2009, **11**, 1724–1727; (c) L. Guadagnini, A. Maljusch, X. Chen, S. Neugebauer, D. Tonelli and W. Schumann, *Electrochim. Acta*, 2009, **54**, 3753–3758.
- 27 C. Reyes-Valerio, *De Bonampak al Templo Mayor: el azul Maya en Mesoamérica*, Siglo XXI, México, 1993.
- 28 N. Yasarawan and J. S. van Duijneveldt, *Langmuir*, 2008, **24**, 7184–7192.
- 29 (a) S. M. G. Pires, R. de Paula, M. M. Q. Simoes, A. M. S. Silva, M. R. M. Domingues, I. C. M. S. Santos, M. D. Vargas, V. F. Ferreira, M. G. P. M. S. Neves and J. A. S. Cavaleiro, *RSC Adv.*, 2011, **1**, 1195; (b) M. Niheues, V. P. Barros, F. d. S. Emery, M. Dias-Baruffi, M. d. D. Assis and N. P. Lopes, *Eur. J. Med. Chem.*, 2012, **54**, 804.
- 30 (a) P. A. L. Ferraz, F. C. de Abreu, A. V. Pinto, V. Glezer, J. Tonholo and M. O. F. Goulart, *J. Electroanal. Chem.*, 2001, **507**, 275–286; (b) F. C. de Abreu, M. O. F. Goulart and A. M. Oliveira-Brett, *Electroanalysis*, 2002, **14**, 29–34; (c) E. Ngameni, I. K. Tonle, C. P. Nansu and R. Wandji, *Electroanalysis*, 2000, **12**, 847–852; (d) M. O. F. Goulart, N. M. F. Lima, A. E.-G. Sant'Ana, P. A. L. Ferraz, J. C. M. Cavalcanti, P. Falkowski, T. Ossowski and A. Liwo, *J. Electroanal. Chem.*, 2004, **566**, 25–29.
- 31 I. Jungbluth, I. Rühling and W. Ternes, *J. Chem. Soc., Perkin Trans. 2*, 2000, 1946–1952.
- 32 (a) E. Caamal-Fuentes, L. W. Torres-Tapia, P. Simá-Polanco, S. R. Peraza-Sánchez and R. Moo-Puc, *J. Ethnopharmacol.*, 2011, **135**, 719–724; (b) D. E. Arnold, B. F. Bohor, H. Neff, G. M. Feinman, P. R. Williams, L. Dussubieux and R. Bishop, *J. Archaeol. Sci.*, 2012, **39**, 2252–2260.